ELSEVIER

Journal of Chromatography A, 888 (2000) 251–266

JOURNAL OF CHROMATOGRAPHY A

www.elsevier.com/locate/chroma

Separation of acidic solutes by nonaqueous capillary electrophoresis in acetonitrile-based media
Combined effects of deprotonation and heteroconjugation

Joe L. Miller[a,1], Damian Shea[b], Morteza G. Khaledi[a,*]

[a]*Department of Chemistry, North Carolina State University, P.O. Box 8204, Raleigh, NC 27695-8204, USA*
[b]*Department of Toxicology, N.C.S.U., Raleigh, NC 27695, USA*

Received 30 August 1999; received in revised form 28 March 2000; accepted 11 April 2000

Abstract

Nonaqueous capillary electrophoresis (NACE) is a chemical separation technique that has grown in popularity over the past few years. In this report, we focus on the combination of heteroconjugation and deprotonation in the NACE separation of phenols using acetonitrile (ACN) as the buffer solvent. By preparing various dilute buffers consisting of carboxylic acids and tetrabutylammonium hydroxide in ACN, selectivity may be manipulated based on a solute's dissociation constant as well as its ability to form heterogeneous ions with the buffer components. ACN's low viscosity, coupled with its ability to allow for heteroconjugation, often leads to rapid and efficient separations that are not possible in aqueous media. In this report, equations are derived showing the dependence of mobility on various factors, including the pK_a of the analyte, the pH and concentration of the buffer, and the analyte–buffer heteroconjugation constant (K^f). The validity of these equations is tested as several nitrophenols are separated at different pH values and concentrations. Using nonlinear regression, the K^f values for the heteroconjugate formation between the nitrophenols and several carboxylate anions are calculated. Also presented in this report are the NACE separations of the 19 chlorophenol congeners and the 11 priority pollutant phenols (used in US Environmental Protection Agency methods 604, 625/1625 and 8270B).

Keywords: Nonaqueous capillary electrophoresis; Deprotonation; Heteroconjugation; Selectivity; Electrophoretic mobility; Phenols; Chlorophenols; Nitrophenols

1. Introduction

For many applications in chemical analysis, nonaqueous media serve important roles. In capillary electrophoresis (CE), for example, a number of research groups have shown that nonaqueous media often compare favorably with aqueous systems in the separation of both charged and uncharged species (for a recent review of nonaqueous CE methods see Ref. [1]). Acetonitrile (ACN) is one of several solvents that have been employed in nonaqueous capillary electrophoresis (NACE), and researchers have found that ACN's low viscosity coupled with its moderately low polarity makes this solvent particularly useful for separating a variety of solutes. They have shown that the efficiency, selectivity, and

*Corresponding author. Tel.: +1-919-515-2943; fax: +1-919-515-2545.

E-mail address: morteza_khaledi@ncsu.edu (M.G. Khaledi).

[1]Current address: Catalytica, Analytical Research and Development, Greenville, NC 27835, USA.

0021-9673/00/$ – see front matter
PII: S0021-9673(00)00467-2

speed of the separations achieved in this solvent often surpass those obtained in aqueous media.

In 1984, Walbroehl and Jorgenson first reported the use of ACN in NACE as they separated several model compounds in a coal tar fraction [2]. In the past few years, a number of other studies have been performed using ACN as a NACE solvent, both with and without cosolvents. These include the separations of cationic [3–9], anionic [10,11], and neutral [12–17] solutes.

Recently, Okada found that phenols, alcohols, and carboxylic acids could be separated by CE through the formation of heteroconjugates between certain buffer anions (such as perchlorate and chloride) and the undissociated analytes [18,19]. Such formation was shown to occur only in solvents such as ACN that are incapable of forming strong hydrogen bonds with the surrounding molecules. It was discovered that these Brønsted acids could be separated according to the degree to which they formed heteroconjugates with the anion. The electrophoretic mobilities of the heteroconjugates that were measured led to the determination of the heteroconjugate formation constants. It was found that the magnitude of these constants depended on various electron induction factors, as described by Hammett or pK_a values.

The original discovery of conjugate formation between an undissociated acid and an anion was made in the 1950s by French and Roe [20], who performed conductance studies that not only showed picric acid (2,4,6-trinitrophenol) undergoing simple dissociation:

$$HPi \rightleftharpoons H^+ + Pi^- \quad (1)$$

but suggested that a ''triple ion'' also forms:

$$HPi + Pi^- \rightleftharpoons HPi_2^- \quad (2)$$

In the 1960s, triple ions of this type became known as ''homoconjugates'' as several researchers used conductance and potentiometric measurements to evaluate the formation constants of a number of these conjugated ions. It was shown that phenols (among other classes of ionizable compounds) are capable of forming homoconjugates in ACN, not only of the type HA_2^-, but also higher-order conjugates such as $H_2A_3^-$, $H_3A_4^-$, etc. [21–25]. It was also shown that if two or more different acids are present, ''heteroconjugate'' formation can occur, as well:

$$nRH + A^- \rightleftharpoons (RH)_nA^- \quad (3)$$

where $n = 1,2,\ldots$ and RH is a weaker acid than HA [26]. The formation of homo- and heteroconjugates does not occur in protic solvents because the degree of hydrogen bonding in these solvents prevents the association of the dissolved species with one another.

In situations where a nonaqueous electrophoretic buffer contains a deprotonated acid, the resulting anion may form a heteroconjugate with an undissociated acidic solute, thus imparting a negative charge to a solute that would otherwise remain uncharged. In light of the fact that many of the organic acids studied by Okada can be separated in ACN-based media either as deprotonated species or as heteroconjugates, the question arises concerning the CE separation of these analytes using the combined effects of deprotonation and heteroconjugation. This possibility is investigated in this work as several classes of phenols are separated using ACN-based buffers. Also, the influence of some of the properties of the ACN-based buffers on the behavior of these analytes is examined as they migrate under electrophoretic conditions.

2. Experimental

2.1. Apparatus

All separations were performed on a Beckman P/ACE System 5500 instrument (Fullerton, CA, USA). The system was comprised of a 0–30 kV high-voltage built-in power supply, a photodiode array UV detector, and GOLD software for system control and data handling. The capillary was obtained from Polymicro Technologies (Tucson, AZ, USA) and had an internal diameter of 53 μm and an outer diameter of 365 μm. The total length of the capillary was 57 cm (50 cm effective length). The temperature was controlled using a fluorocarbon-based cooling fluid obtained from 3M (St. Paul, MN, USA). All experiments were performed at room temperature. The electropherograms were collected and processed on an IBM PS/2 Model 40 SX

computer. Elution times were compiled and mobilities were calculated in spreadsheet format using Quattro Pro for Windows Version 6.02 (Novell, Atlanta, GA, USA), and nonlinear regression calculations were performed using SAS software (Cary, NC, USA).

2.2. Reagents and chemicals

HPLC-grade acetonitrile and glacial acetic acid were obtained from Fisher Scientific (Raleigh, NC, USA), the dicarboxylic acids and 1 *M* tetrabutylammonium hydroxide (TBAH) in methanol were obtained from Aldrich (Milwaukee, WI, USA), and the test phenols were obtained from Aldrich and Chem Service (West Chester, PA, USA).

2.3. Procedure

The pH values of the buffer solutions prepared in this study were not measured potentiometrically. Rather, the pH values of these solutions were taken to be equal to the published pK_a values as a given number of millimoles of weak acid was dissolved in ACN followed by half the number of millimoles of strong base (TBAH). This resulted in a weak acid–conjugate base (1:1) buffer, which was then filtered through a 0.45-μm Gelman nylon aerodisk filter. Concentrated stock solutions (1 mg/ml) of individual test solutes were prepared in ACN. The injected samples were prepared by transferring a measured aliquot of the stock solution containing the desired solute into an autosampler vial, adding pyrene (the electroosmotic flow marker), and diluting with ACN to a final concentration of 25 μg/ml.

At the beginning of the day, the capillary was flushed with 1 *M* sodium hydroxide for 2 min, followed by deionized water for 2 min. Prior to each run, the capillary was equilibrated with the run buffer for 2 min. All samples were injected for 1 s using the pressure injection mode. The applied voltage was 25 kV (30 kV for some runs) and was unchanged for the duration of each run; this yielded currents ranging from 2.0 to 20 μA. The absorbance detector wavelength was set at 214 nm.

The electrophoretic mobilities were calculated using the equation:

$$\mu_{ep} = \frac{L_t L_d}{V} \cdot \left(\frac{1}{t_r} - \frac{1}{t_{eo}} \right) \quad (4)$$

where L_t is the total length of the capillary, L_d is the effective length (i.e., distance between points of injection and detection) of the capillary, t_r represents the migration time of the solute, t_{eo} is the migration time due solely to electroosmotic flow, and V is the applied voltage across the capillary.

3. Results and discussion

3.1. Effect of buffer pH on mobility

In many studies that employ aqueous buffers in standardizing pH electrodes, the term ''apparent pH'' (or pH*) is used in dealing with nonaqueous solutions due to the uncertainties in the liquid-junction potential of the glass electrode as it is transferred from an aqueous to a nonaqueous medium. On the other hand, when the term ''pH'' (rather than pH*) is used in the context of nonaqueous media, it is generally more theoretical in scope and is usually reserved for expressing hydrogen-ion activities that are calculated from thermodynamically-derived pK_a values. As an example, Kolthoff uses the quantity ''pH–pK_a'' as an independent variable to show changes in the buffer capacity profile of a nonaqueous solution at various buffer concentrations [27]. In our report, the term ''pH'' is likewise used, but only as a theoretical quantity based on previously-published pK_a values. Also, it should be pointed out that as a matter of simplicity, concentrations rather than activities are used in the equilibrium expressions listed in this report.

In this study, all of the separations of the phenol mixtures in ACN-based media were achieved in less than 10 min. This is illustrated in Fig. 1, in which several nitrophenols were separated using a buffer consisting of 40 m*M* succinic acid and 20 m*M* TBAH in ACN. The short run times were attributed primarily to the relatively high dielectric constant/viscosity ratio of ACN. This separation stems from the combination of two factors: simple deprotonation and the formation of heteroconjugates between the analytes and the buffer components. In Fig. 1, the first five phenols that eluted have pK_a values ranging

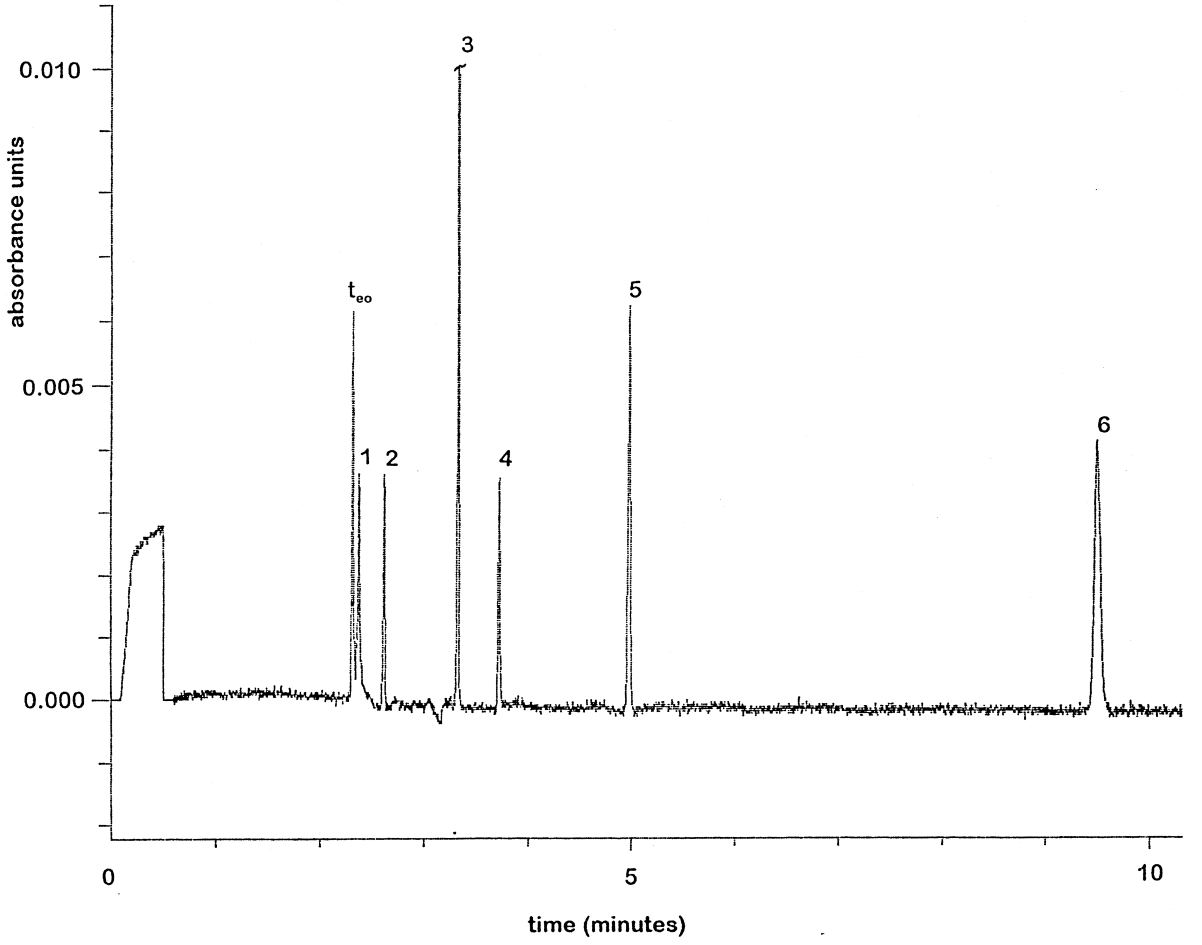

Fig. 1. Separation of nitrophenols in 40 m*M* succinic acid+20 m*M* TBAH in ACN. 30 kV→20 μA. Peak identification: (1) 2-nitrophenol, (2) phenol, (3) 3-nitrophenol, (4) 4-nitrophenol, (5) 3,5-dinitrophenol, (6) 2,4-dinitrophenol.

from 20.5 to 27.2 (see Table 1), several units higher than the pH of the bisuccinate buffer (17.6, see Table 2). Only 2,4-dinitrophenol (the last solute to elute) had a pK_a lower than the buffer pH. When this separation was attempted in an aqueous system, these conditions resulted in the isolation of 2,4-dinitrophenol, with the remaining analytes coeluting with the electroosmotic flow. As Fig. 2 shows, a large decrease in mobility was observed even when small amounts (up to 10%) water was added to an ACN-based buffer.

In aqueous CE, the following equation may be used to predict the mobility of a solute (RH) at a given pH:

Table 1
pK_a values of selected phenols [26]

Compound	pK_a in ACN	pK_a in water
Phenol	27.2	9.99
2-Nitrophenol	22.1	7.23
3-Nitrophenol	23.8	8.0
4-Nitrophenol	20.9	7.15
2,4-Dinitrophenol	16.0	4.0
3,5-Dinitrophenol	20.5	6.7
3-Chlorophenol	25.04	9.1
4-Chlorophenol	25.44	9.4
3,4-Dichlorophenol	24.06	8.6
3,5-Dichlorophenol	23.31	8.2
3,4,5-Trichlorophenol	22.54	7.8

Table 2
Buffers prepared for the mobility study of nitrophenols at various pH values in ACN

Weak acid	Chemical formula	pH in ACN [26]	Concentration (m*M*)	
			Acid	TBAH
Oxalic	HOOCCOOH	14.5 (pK_{a1})	10.00	5.00
Malonic	$HOOCCH_2COOH$	15.3 (pK_{a1})	10.00	5.00
Succinic	$HOOC(CH_2)_2COOH$	17.6 (pK_{a1})	10.00	5.00
Glutaric	$HOOC(CH_2)_3COOH$	19.2 (pK_{a1})	10.00	5.00
Adipic	$HOOC(CH_2)_4COOH$	20.4 (pK_{a1})	10.00	5.00
Acetic	CH_3COOH	22.3 (pK_a)	10.00	5.00
Azelaic	$HOOC(CH_2)_7COOH$	24.8 (pK_{a2})	2.50	3.75
Adipic	$HOOC(CH_2)_4COOH$	26.9 (pK_{a2})	2.50	3.75
Malonic	$HOOCCH_2COOH$	30.5 (pK_{a2})	2.50	3.75
(None)		~35	–	5.00

$$\mu_{ep} = \frac{K_a}{[H^+] + K_a} \cdot \mu_{R^-} \quad (5)$$

where K_a is dissociation constant of the solute, $[H^+]$ is the hydrogen-ion concentration, and μ_{R^-} is the mobility of the fully deprotonated form of RH. In plotting mobility vs. pH for a solute, a sigmoidal curve is obtained with an inflection point where the buffer pH is equal to the pK_a of the solute. At pH values greater or less (typically ±2 units) than the solute's pK_a, the mobility reaches a limiting value: zero if the solute is completely undissociated, and the maximum mobility if the solute is fully ionized. Such plots have been useful in predicting the migration behavior of a number of solute classes. In our laboratory, it was previously shown that the information gathered from mobility-vs.-pH curves could be used in the optimization of the pH that provided maximum selectivity for a set of substituted phenols [28].

Under nonaqueous conditions, however, similar sigmoidal curves may or may not be obtained

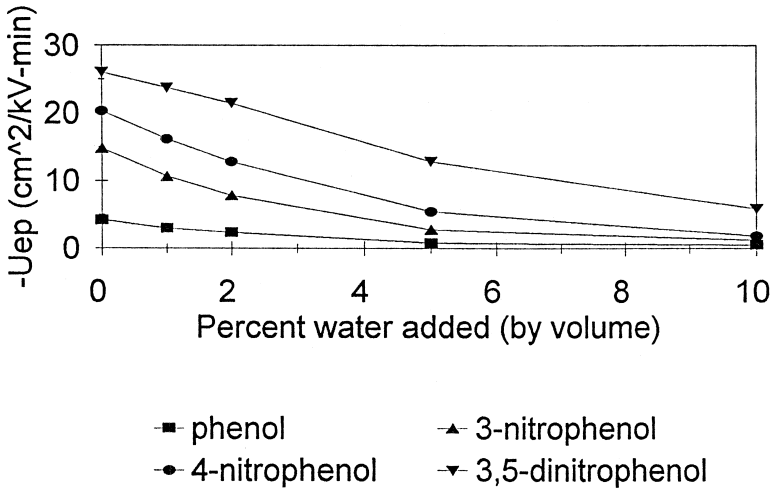

Fig. 2. Loss of heteroconjugation upon addition of water to a buffer containing 20 m*M* adipic + 10 m*M* TBAH in ACN. Square = phenol, triangle = 3-nitrophenol, circle = 4-nitrophenol, and inverted triangle = 3,5-dinitrophenol.

depending on the nature of the solvent. It was previously shown [29] that the sigmoidal behavior is observed in *N*-methylformamide (a moderately polar protic solvent) using a buffer that consisted of 3-cyclohexyl-1-propanesulfonic acid (CAPS) and TBAH.

In this project with ACN, we used buffers from several different weak acids (listed in Table 2) and added TBAH so that $pH = pK_a$ in all cases. All of these acids (with the exception of acetic acid) were dicarboxylic acids with pK_a values ranging from 14.5 to 30.5 in ACN, and all buffers were prepared using the appropriate amounts of acid and TBAH so that a constant ionic strength between buffers could be maintained. The mobilities of the nitrophenols were then measured in each buffer, and a plot of mobility as a function of pH for each phenol was constructed (Fig. 3). The plot that would be generated in the absence of heteroconjugation (according to Eq. (5)) is shown as a solid curve for each solute. In this curve, the limiting mobility of the solute was assumed to be its mobility in unbuffered TBAH, the estimated $pH \cong 35$ of which was based on data collected by Parekh and Rogers [30]. The measured values, on the other hand deviate, significantly in some cases, from the theoretical curve due to the effects of heteroconjugation. A notable exception to this trend occurs in certain phenols such as 2-nitrophenol (Fig. 3B) where one or more substituents are positioned adjacent to the hydroxyl moiety on the ring. In this case, intramolecular hydrogen bonding takes place (the so-called ''*ortho* effect''), thus greatly inhibiting the formation of heteroconjugates with the surrounding species. Especially interesting is the observation that heteroconjugation seems to increase with the buffer pK_a, even though the pH remains several units below the pK_a of the analyte. This should not be surprising, however, since for the dicarboxylic acids, an increase in the carbon-chain length increases the pK_a of the molecule. Since weak acids with higher pK_a values give rise to stronger conjugate bases (the species actually responsible for heteroconjugation with the neutral analyte), the mobility that is gained through heteroconjugation increases, as well.

3.2. Effect of buffer concentration on mobility

In general, the net electrophoretic mobility (μ_{ep}) of an acidic solute (RH) that undergoes heteroconjugation and/or deprotonation may be expressed as follows:

$$\mu_{ep} = \sum_i \alpha_i \mu_i \tag{6}$$

In this equation, α_i and μ_i represent the molar fraction and mobility of species *i*, respectively, with *i* referring to any form of R that is present in solution. In an aprotic solvent such as ACN, R may exist in one of several forms: as the undissociated acid (RH), as the deprotonated acid (R^-), as $(RH)_nA^-$ in which RH forms a heteroconjugate with a deprotonated buffer component (A^-):

$$nRH + A^- \rightleftharpoons (RH)_nA^- \tag{7}$$

or as $R(HA)_n^-$ arising from the heteroconjugation of R^- with the protonated buffer component (HA):

$$R^- + nHA \rightleftharpoons R(HA)_n^- \tag{8}$$

In Eq. (6), it may be assumed that RH, being uncharged, possesses no mobility of its own, and therefore makes no contribution to the overall mobility. Furthermore, because of the low concentrations of analyte and buffer used in this study, it may be possible to neglect the formation of heteroconjugates other than RHA^- [i.e., $(RH)_nA^-$ and $R(HA)_n^-$, where $n = 1$]. Thus, Eq. (6) may be expanded as follows:

$$\mu_{ep} = \alpha_{R^-}\mu_{R^-} + \alpha_{RHA^-}\mu_{RHA^-} \tag{9}$$

where μ_{R^-} and μ_{RHA^-} represent the limiting mobilities of R^- and RHA^-, respectively, while:

$$\alpha_{R^-} = \frac{[R^-]}{[RH] + [R^-] + [RHA^-]} \tag{10}$$

and

$$\alpha_{RHA^-} = \frac{[RHA^-]}{[RH] + [R^-] + [RHA^-]} \tag{11}$$

In Eqs. (10) and (11), $[R^-]$ may be expressed as:

$$[R^-] = \frac{K_a[RH]}{[H^+]} \tag{12}$$

while $[RHA^-]$ involves a similar relationship based on the heteroconjugation constant, $K^f_{RHA^-}$. One must remember, however, that the formation of RHA^- can

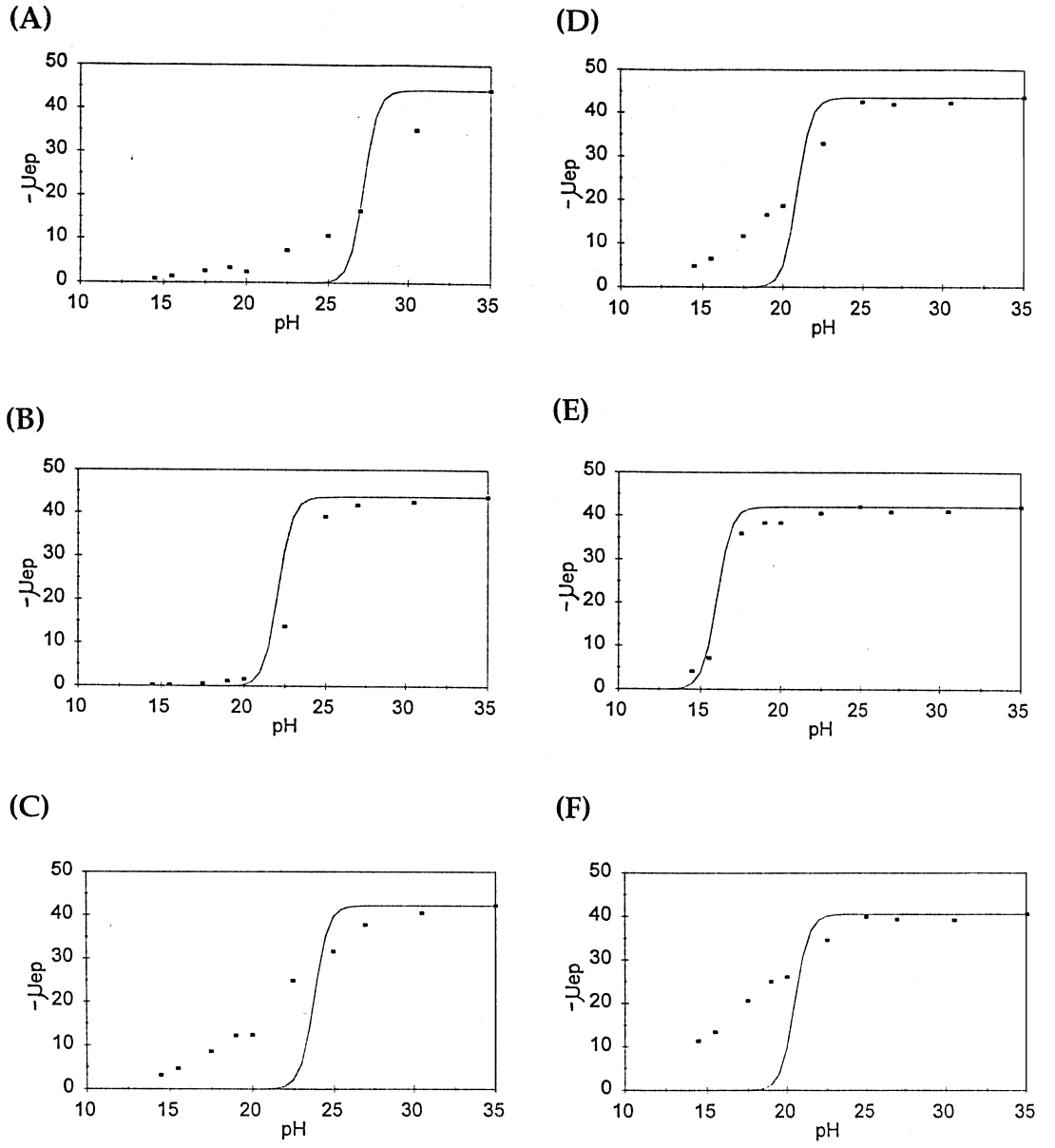

Fig. 3. Observed mobility of nitrophenols as a function of buffer pH. The curves show the expected behavior according to Eq. (5). (A) Phenol, (B) 2-nitrophenol, (C) 3-nitrophenol, (D) 4-nitrophenol, (E) 2,4-dinitrophenol, and (F) 3,5-dinitrophenol.

occur through two different pathways (Eqs. (7) and (8)), so that:

$$[RHA^-] = [(RH)A^-] + [R(HA)^-] \quad (13)$$

Eqs. (7) and (8) (with $n=1$) thus give rise to two distinct formation constants:

$$K^{f}_{(RH)A^-} = \frac{[(RH)A^-]}{[RH][A^-]} \quad (14)$$

and

$$K^{f}_{R(HA)^-} = \frac{[R(HA)^-]}{[R^-][HA]} \quad (15)$$

Eqs. (12–15) may be substituted into Eq. (10) to obtain:

$$\alpha_{R^-} = \frac{\frac{K_a[RH]}{[H^+]}}{[RH] + \frac{K_a[RH]}{[H^+]} + K^f_{(RH)A^-}[RH][A^-] + K^f_{R(HA)^-}\frac{K_a[RH]}{[H^+]}[HA]} \quad (16)$$

which simplifies to:

$$\alpha_{R^-} = \frac{K_a}{[H^+] + K_a + K^f_{(RH)A^-}[H^+][A^-] + K^f_{R(HA)^-}K_a[HA]} \quad (17)$$

Likewise, Eq. (11) becomes:

$$\alpha_{RHA^-} = \frac{K^f_{(RH)A^-}[RH][A^-] + K^f_{R(HA)^-}\frac{K_a[RH]}{[H^+]}[HA]}{[RH] + \frac{K_a[RH]}{[H^+]} + K^f_{(RH)A^-}[RH][A^-] + K^f_{R(HA)^-}\frac{K_a[RH]}{[H^+]}[HA]} \quad (18)$$

simplifying to:

$$\alpha_{RHA^-} = \frac{K^f_{(RH)A^-}[H^+][A^-] + K^f_{R(HA)^-}K_a[HA]}{[H^+] + K_a + K^f_{(RH)A^-}[H^+][A^-] + K^f_{R(HA)^-}K_a[HA]} \quad (19)$$

Substituting Eqs. (17) and (19) into Eq. (9), therefore, gives the following general equation:

$$\mu_{ep} = \frac{K_a\mu_{R^-} + \left(K^f_{(RH)A^-}[H^+][A^-] + K^f_{R(HA)^-}K_a[HA]\right)\mu_{RHA^-}}{[H^+]\left(K^f_{(RH)A^-}[A^-] + 1\right) + K_a\left(K^f_{R(HA)^-}[HA] + 1\right)} \quad (20)$$

From Eq. (20), a series of plots may be constructed to show the theoretical dependence of mobility on buffer concentration under various conditions. Some of these plots are shown in Fig. 4, in which several special cases are considered:

(1) If the pH of the separation buffer remains several units below the pK_a of the analyte (i.e., $[H^+] >> K_a$), then the mobility depends solely on the heteroconjugation between RH and A^-. The K_a terms drop, and Eq. (20) reduces to:

$$\mu_{ep} = \frac{K^f_{(RH)A^-}[A^-]}{K^f_{(RH)A^-}[A^-] + 1} \cdot \mu_{RHA^-} \quad (21)$$

In this case, if the buffer concentration (as described by $[A^-]$) approaches zero, then μ_{ep} also approaches zero. At high concentrations, however, μ_{ep} approaches μ_{RHA^-}. Curve A of Fig. 4 shows this behavior.

(2) If the pH of the separation buffer lies several

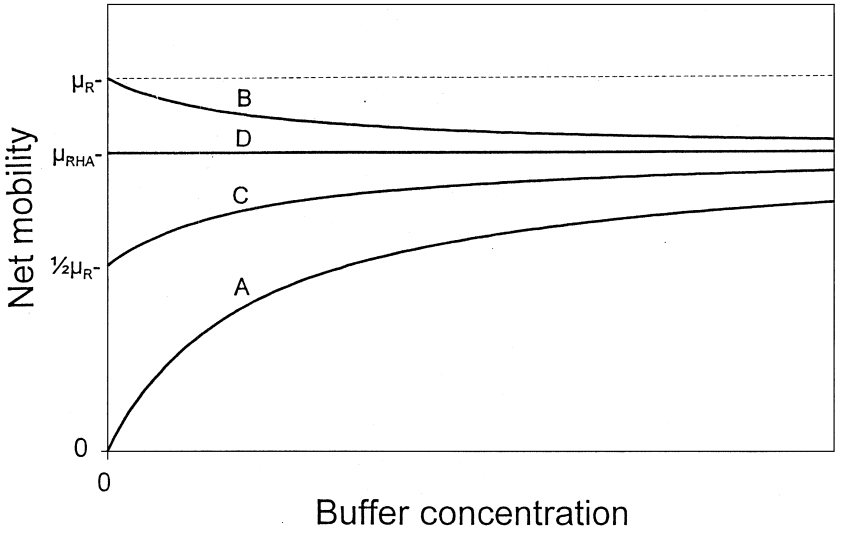

Fig. 4. Theoretical dependence of mobility on buffer concentration in ACN when (A) pH<<pK_a, (B) pH>>pK_a, (C) pH=pK_a, and (D) pH=pK_a − log $[(\mu_{R^-}/\mu_{RHA^-}) - 1]$.

units above the pK_a of the analyte (i.e., $[H^+] << K_a$), then the mobility-vs.-buffer concentration ([HA]) relationship depends on the contributions from R^- and $R(HA)^-$. The $[H^+]$ terms drop, so that Eq. (20) becomes:

$$\mu_{ep} = \frac{\mu_{R^-} + K^f_{R(HA)^-}[HA]\mu_{RHA^-}}{K^f_{R(HA)^-}[HA] + 1} \quad (22)$$

a plot of which resembles curve B in Fig. 4. Note that as zero buffer concentration is approached, the mobility approaches the limiting mobility of R^- (μ_{R^-}), whereas at high buffer concentrations, μ_{RHA^-} is approached.

(3) When the pK_a of the analyte is equal to the pH of the buffer (i.e., $[H^+] = K_a$), Eq. (20) reduces to:

$$\mu_{ep} = \frac{\mu_{R^-} + \left(K^f_{(RH)A^-}[A^-] + K^f_{R(HA)^-}[HA]\right)\mu_{RHA^-}}{K^f_{(RH)A^-}[A^-] + K^f_{R(HA)^-}[HA] + 2} \quad (23)$$

According to this equation, μ_{ep} approaches $1/2\mu_{R^-}$ at very low buffer concentrations (i.e., $[A^-]+[HA]$), while at high concentrations, μ_{ep} approaches μ_{RHA^-}. Curve C of Fig. 4 illustrates this behavior.

Table 3 summarizes the effects of pH and buffer concentration in cases 1–3.

(4) In the cases discussed so far, the net mobility approaches μ_{RHA^-} at high buffer concentrations. For a given analyte and buffer type, however, there exists a unique pH at which μ_{ep} is equal to μ_{RHA^-} for all buffer concentrations, as curve D of Fig. 4 depicts. This occurs when:

$$pH = pK_a - \log\left(\frac{\mu_{R^-}}{\mu_{RHA^-}} - 1\right) \quad (24)$$

which is derived by setting μ_{ep} equal to μ_{RHA^-} in Eq. (9).

(5) All of the special cases described above pertain only to certain aprotic media where heteroconjugation can take place. In the presence of protic solvents (such as water), though, heteroconjugation cannot occur, and Eq. (20) simplifies to:

$$\mu_{ep} = \frac{K_a}{[H^+] + K_a} \cdot \mu_{R^-} \quad (25)$$

To test the validity of Eq. (20) (or simplifications thereof), the solutes separated in Fig. 1 were injected at several concentrations of an acetic acid–acetate (1:1) buffer. The mobilities of each solute were then plotted against the buffer concentration, to which a nonlinear curve was fit using nonlinear regression. In this procedure, known $[H^+]$ and/or K_a values were substituted into the appropriate equation, and through an iterative algorithm, a curve was fit to the data points so that the sum of the squares was minimized. In our case, the pK_a values for phenol (27.2) and 3-nitrophenol (23.8) were higher than the pH of the acetate buffer (22.3), while the pK_a values for 2,4-dinitrophenol (16.0) and 3,5-dinitrophenol (20.5) were several units lower than the buffer pH. For these solutes, Eqs. (21) and (22), respectively, were used to fit the mobility data. However, for the remaining nitrophenols (whose pK_a values approach that of acetic acid), the general form of the equation (Eq. (20)) was used. The mobility data points for the nitrophenols separated in the acetate buffer, as well as the best fitting curves, are shown in Fig. 5. Not surprisingly, the plots for phenol and 3-nitrophenol resemble curve A in Fig. 4 (even though 3-nitrophenol is partially deprotonated), whereas the plots for 2,4-dinitrophenol and 3,5-dinitrophenol resemble curve B. On the other hand, the plot for 2-nitro-

Table 3
Effect of pH and buffer concentration on the mobility of a weakly acidic solute

If:	and:	then:	and:	therefore:
$pH << pK_a$	$[A^-] \to 0$	$\alpha_{R^-} \to 0$	$\alpha_{RHA^-} \to 0$	$\mu \to 0$
$pH << pK_a$	$[A^-] \to \infty$	$\alpha_{R^-} \to 0$	$\alpha_{RHA^-} \to 1$	$\mu \to \mu_{RHA^-}$
$pH >> pK_a$	$[HA] \to 0$	$\alpha_{R^-} \to 1$	$\alpha_{RHA^-} \to 0$	$\mu \to \mu_{R^-}$
$pH >> pK_a$	$[HA] \to \infty$	$\alpha_{R^-} \to 0$	$\alpha_{RHA^-} \to 1$	$\mu \to \mu_{RHA^-}$
$pH = pK_a$	$[A^-]+[HA] \to 0$	$\alpha_{R^-} \to 0.5$	$\alpha_{RHA^-} \to 0$	$\mu \to 1/2\mu_{R^-}$
$pH = pK_a$	$[A^-]+[HA] \to \infty$	$\alpha_{R^-} \to 0$	$\alpha_{RHA^-} \to 1$	$\mu \to \mu_{RHA^-}$

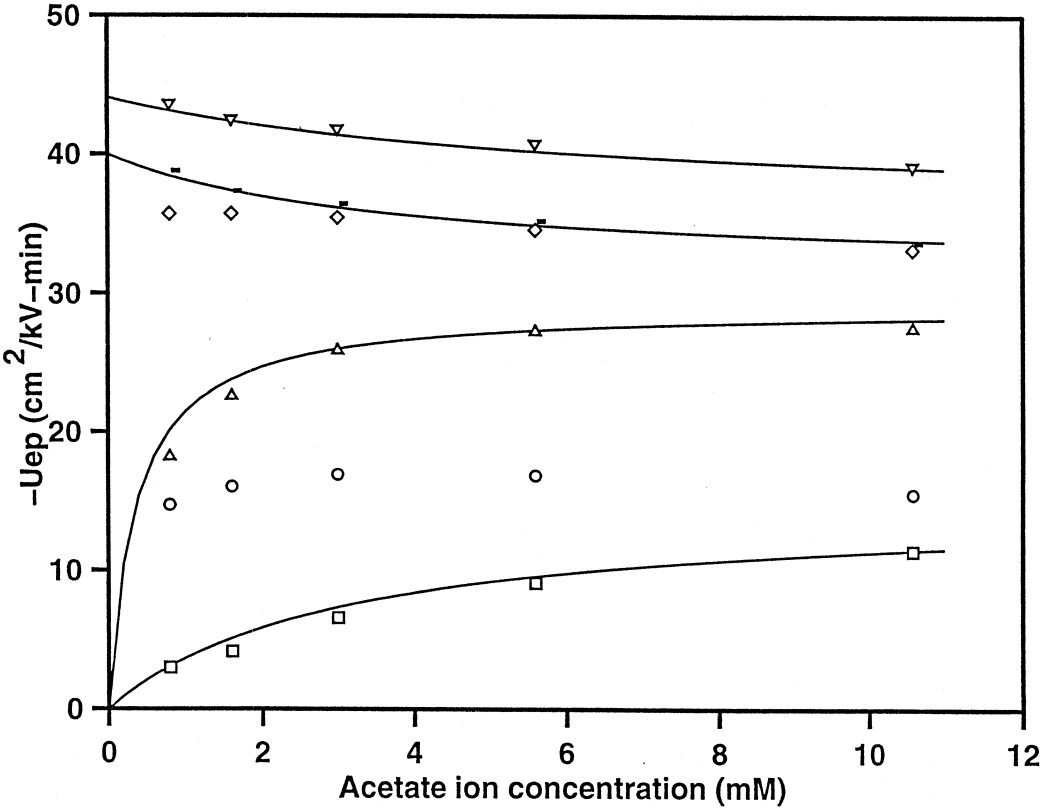

Fig. 5. Observed and calculated mobilities of nitrophenols as a function of acetate ion concentration [in an acetic acid–acetate (1:1) buffer in ACN]. Circle = 2-nitrophenol, square = phenol, triangle = 3-nitrophenol, diamond = 4-nitrophenol, dash = 3,5-dinitrophenol, and inverted triangle = 2,4-dinitrophenol.

phenol (the pK_a of which lies close to the buffer pH) shows similarity to curve C, and the plot for 4-nitrophenol (whose mobility changes little with buffer concentration) bears resemblance to curve D. For these two mononitrophenols, deviations from ideality (see below) were observed in the mobility-vs.-concentration plots, and when we attempted to fit these data points to Eq. (20), the data failed to converge. Therefore, the curves that best fit these points are not shown in Fig. 5.

A series of plots similar to those generated in Fig. 5 were also made for the nitrophenols separated in the bisuccinate buffer (Fig. 6). In this case, all of the solutes were fit to Eq. (21), except for 2,4-dinitrophenol, which was fit to Eq. (22).

Under certain buffer conditions, the analytes remain protonated, and thus derive their mobilities from the formation of heteroconjugates with the charged buffer components. For these solutes under such conditions, the heteroconjugate formation constant [$K^{f}_{(RH)A^-}$] and the limiting mobilities of the heteroconjugate (μ_{RHA^-}) may be evaluated based on the nonlinear fit using Eq. (20). Table 4 lists the $K^{f}_{(RH)A^-}$ and μ_{RHA^-} values (as well as their standard errors) of the nitrophenols and selected chlorophenols that remain protonated under various buffer conditions.

For a given buffer, there seemed to be a parallel between the $K^{f}_{(RH)A^-}$ values obtained for the protonated phenols and the mobilities of these solutes. This was to be expected since the heteroconjugation properties of a solute is determined primarily by the solute's ability to interact with the dissociated buffer components through hydrogen bonding, which, in turn, is linked to the number and position of electron-withdrawing groups on the solute molecule.

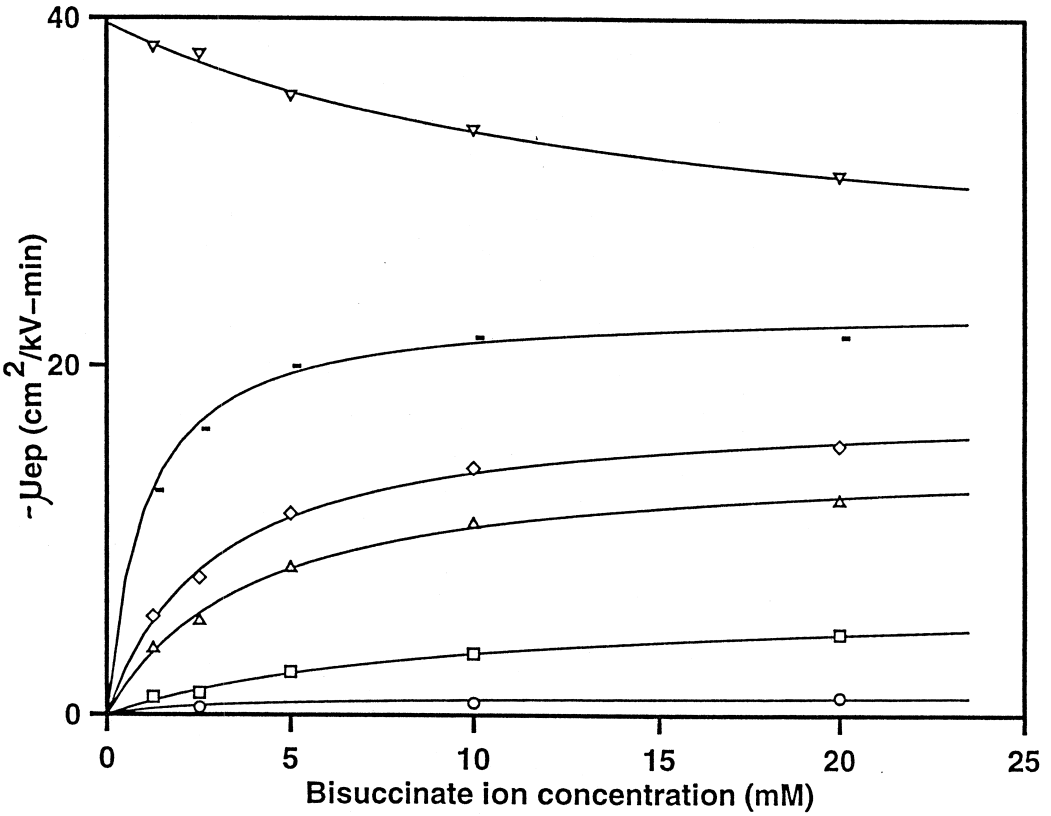

Fig. 6. Observed and calculated mobilities of nitrophenols as a function of bisuccinate ion concentration [in a succinic acid–bisuccinate (1:1) buffer in ACN]. Legend the same as in Figs. 3–6.

Table 5 shows the mobilities of a series of substituted phenols, which were separated in a buffer containing 5 m*M* succinic acid–5 m*M* bisuccinate in ACN. Of these, only 2,4-dinitrophenol and possibly the tetra- and pentachlorophenols become at least partially deprotonated at pH 17.6 (thus gaining their own mobilities). In all other cases, the mobility is imparted through heteroconjugate formation. If the phenol ring contains one or more electron-withdrawing groups (i.e., nitro, halo, or carboxyl groups) then the degree of heteroconjugation increases relative to that of unsubstituted phenol, and the mobility increases, as well (except for 2-nitrophenol and 2,4-dinitrophenol, which demonstrate the ''*ortho* effect''). If, however, electron-releasing alkyl groups are present, then the degree of heteroconjugation is reduced relative to phenol, thus decreasing the mobility.

The limiting mobilities (μ_{RHA^-}) we obtained, on the other hand, were somewhat perplexing. Since heteroconjugates of the type RHA^- all possess a -1 charge, one would expect differences in μ_{RHA^-} values to be derived mainly from differences in solute size and shape, with phenol having the highest μ_{RHA^-}, followed by the monosubstituted phenols, and then the more highly substituted phenols. A comparison of the μ_{RHA^-} values in Table 4, however, shows otherwise. Although the errors associated with these values are generally low (typically less than 10% of the determined μ_{RHA^-}), the magnitude of μ_{RHA^-} seems to parallel the $K^f_{(RH)A^-}$ values. Note that the error in the $K^f_{(RH)A^-}$ are greater for solutes with larger errors in μ_{RHA^-}. Moreover, it was observed that when the mobilities of certain solutes (especially those whose pK_a were near the pH of buffer in use) were measured, the mobility reached a maximum and gradually decreased as the buffer concentration was further increased. An example of

Table 4
Heteroconjugation constants and limiting mobilities (in cm^2/kV min) for selected protonated phenols in an ACN-based buffers, as determined via nonlinear regression[a]

	$K^f_{(RH)A^-}$	μ_{RHA^-}
Oxalic acid/bioxalate		
3-Nitrophenol	791 (299)	4.6 (0.5)
4-Nitrophenol	326 (40)	9.8 (0.5)
2,4-Dinitrophenol	342 (114)	7.9 (1.0)
3,5-Dinitrophenol	487 (65)	20.1 (0.9)
3-Chlorophenol	281 (70)	4.3 (0.4)
3,4-Dichlorophenol	298 (67)	6.5 (0.6)
3,5-Dichlorophenol	327 (34)	8.0 (0.3)
3,4,5-Trichlorophenol	367 (39)	10.3 (0.4)
Succinic acid/bisuccinate		
Phenol	109 (18)	6.8 (0.5)
2-Nitrophenol	166 (108)	1.3 (0.3)
3-Nitrophenol	256 (25)	15.0 (0.5)
4-Nitrophenol	347 (31)	17.9 (0.5)
3,5-Dinitrophenol	993 (99)	23.5 (0.5)
3-Chlorophenol	143 (13)	10.6 (0.5)
3,4-Dichlorophenol	150 (24)	15.3 (1.3)
3,5-Dichlorophenol	185 (18)	17.0 (0.8)
3,4,5-Trichlorophenol	264 (17)	18.8 (0.5)
Adipic acid/biadipate		
Phenol	717 (256)	4.2 (0.4)
3-Nitrophenol	816 (114)	16.7 (0.7)
3-Chlorophenol	556 (103)	10.6 (0.7)
3,4-Dichlorophenol	826 (91)	14.9 (0.5)
3,5-Dichlorophenol	1232 (201)	17.2 (0.7)
3,4,5-Trichlorophenol	1835 (161)	20.5 (0.4)
Acetic acid/acetate		
Phenol	333 (35)	14.7 (0.6)
3-Chlorophenol	1333 (96)	22.4 (0.3)
3,4-Dichlorophenol	2514 (147)	27.2 (0.3)
3,5-Dichlorophenol	4391 (590)	30.0 (0.5)

[a] Standard errors are given in parentheses.

Table 5
Calculated mobilities (in cm^2/kV min) of substituted phenols in a buffer containing 5 m*M* succinic acid–5 m*M* bisuccinate in ACN

2-Nitrophenol	0.62
2,4-Dimethylphenol	1.42
3,5-Dimethylphenol	1.73
2,6-Dichlorophenol	1.93
2-Methylphenol	2.03
4-Ethylphenol	2.05
4-Methylphenol	2.18
3-Methylphenol	2.29
2,4,6-Trichlorophenol	2.95
Phenol	3.07
2,3,6-Trichlorophenol	3.12
4-Chloro-3-methylphenol	3.78
2-Chlorophenol	4.03
4-Iodophenol	4.36
4-Bromophenol	4.53
4-Chlorophenol	5.00
p-Hydroxymethylbenzoate (methyl paraben)	5.04
3-Chlorophenol	5.53
2,3,4,6-Tetrachlorophenol	6.82
2,4-Dichlorophenol	7.11
2,3-Dichlorophenol	7.27
4-Fluorophenol	7.49
3,4-Dichlorophenol	8.23
2,5-Dichlorophenol	9.51
3-Nitrophenol	9.69
3,5-Dichlorophenol	9.85
2,3,4-Trichlorophenol	10.23
2,3,5,6-Tetrachlorophenol	10.64
3,4,5-Trichlorophenol	11.48
2,4,5-Trichlorophenol	11.89
4-Nitrophenol	12.53
2,3,5-Trichlorophenol	12.56
2,3,4,5-Tetrachlorophenol	14.65
Pentachlorophenol	18.37
3,5-Dinitrophenol	19.01
2,4-Dinitrophenol	29.19

this is shown in Fig. 5 where 2-nitrophenol reached a maximum mobility of 16.9 cm^2/kV min at a concentration of 2.5 m*M* acetate, and then dropped to 15.5 cm^2/kV min at the highest buffer concentration (10 m*M*).

There are at least two possible explanations that may account for this behavior, the first of which involves the earlier assumption that only the simplest heteroconjugate (RHA^-) forms under the buffer concentrations used in this study. It is, however, possible that at higher concentrations of buffer, higher-order conjugates may be present, as well. The formation of $R(HA)_2^-$, for example, requires modification to Eq. (20), resulting in a relationship that is quadratic in nature. In this case, a plot of mobility vs. buffer concentration would produce a curve that quickly reaches a maximum mobility and either levels out or slowly decreases at higher buffer concentrations (as was observed with 2-nitrophenol in the acetate buffer).

The second explanation that would account for lower-than-expected μ_{RHA^-} values deals with the decrease in mobility that is generally observed at higher ionic strengths, regardless of the solvent used. The increased interactions between the charged

analytes and the counterion (TBA^+, in this case) results in the formation of an ion pair, which offsets the charge (and hence the mobility) of the anion as it migrates through the electrophoretic medium. In theory, the mobility of a charged analyte should decrease with the square root of the ionic strength of the buffer [31]. In our experiments, this behavior was indeed observed at higher pH values where heteroconjugates were not expected to form. As Fig. 7 shows, the mobility of the deprotonated form of 3-nitrophenol increased as the ACN-based malonate buffer (pH 30.5) was serially diluted. Since this behavior would also be expected at lower pH values where heteroconjugation is present, the changes in ionic strength can also contribute to the leveling of the mobility curves in Fig. 6.

3.3. Separation of chlorophenols and priority pollutants

The CE separation of the nineteen chlorophenol congeners has always proven difficult since many of these compounds are geometric isomers of each other and possess similar pK_a values. Consequently, no purely aqueous CE method has been developed that can separate all 19 congeners [32]. The separation of these compounds, though, was achieved by Otsuka et al. using micellar electrokinetic chromatography (MEKC) [33]. More recently, Zemann and Volgger separated all but two of the chlorophenol congeners using a mixed hydro–organic solvent containing 2-butanol, ethylene glycol and ACN. The use of this medium resulted in the coelectroosmotic separation of the solutes in under 4 min [34]. The separation of all 19 congeners in less than 6 min using a buffer containing 10 m*M* acetic acid and 5 m*M* TBAH in ACN is shown in Fig. 8. This separation produced an elution pattern in which the less-substituted chlorophenol congeners eluted first followed by the more chlorinated congeners, similar to the pattern observed in aqueous CE runs [35]. The reason for the observed elution order may be traced to the electron-withdrawing chlorine groups, which lowers the pK_a values of the phenols (Table 1). Since the degree of dissociation is greater for the heavily-chlorinated phenols at moderate pH values (20–25), these compounds possessed greater mobility in the direction counter to the electroosmotic flow, and thus, they eluted later than the less-dissociated chlorophenols. At higher pH values, however, the elution order reversed as the remaining chlorophenols became fully deprotonated. In this case, the mobility was determined primarily by the mass of the resulting anion, and the larger species (with less mobility) eluted prior to the smaller species. The separation of the chlorophenols presented in Fig. 8

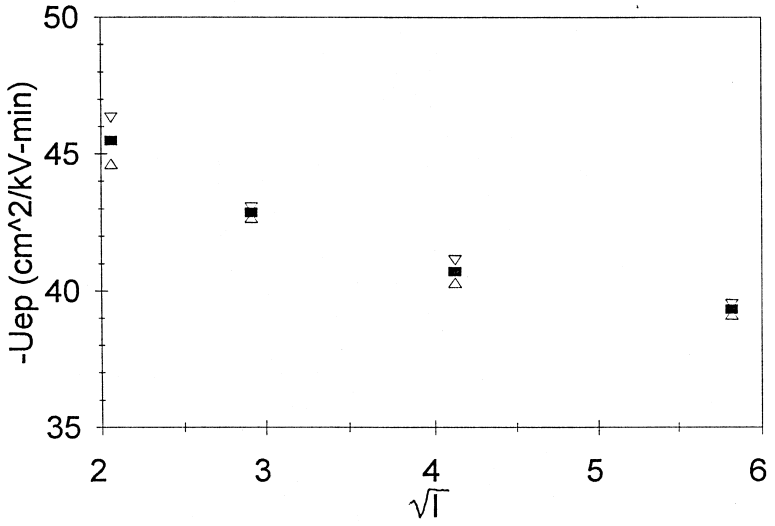

Fig. 7. Dependence of the mobility of 3-nitrophenol on ionic strength in the absence of heteroconjugation. The buffer consisted of malonic acid adjusted to pK_{a2} (30.5) with TBAH in ACN. Ionic strengths are in units of millimolal.

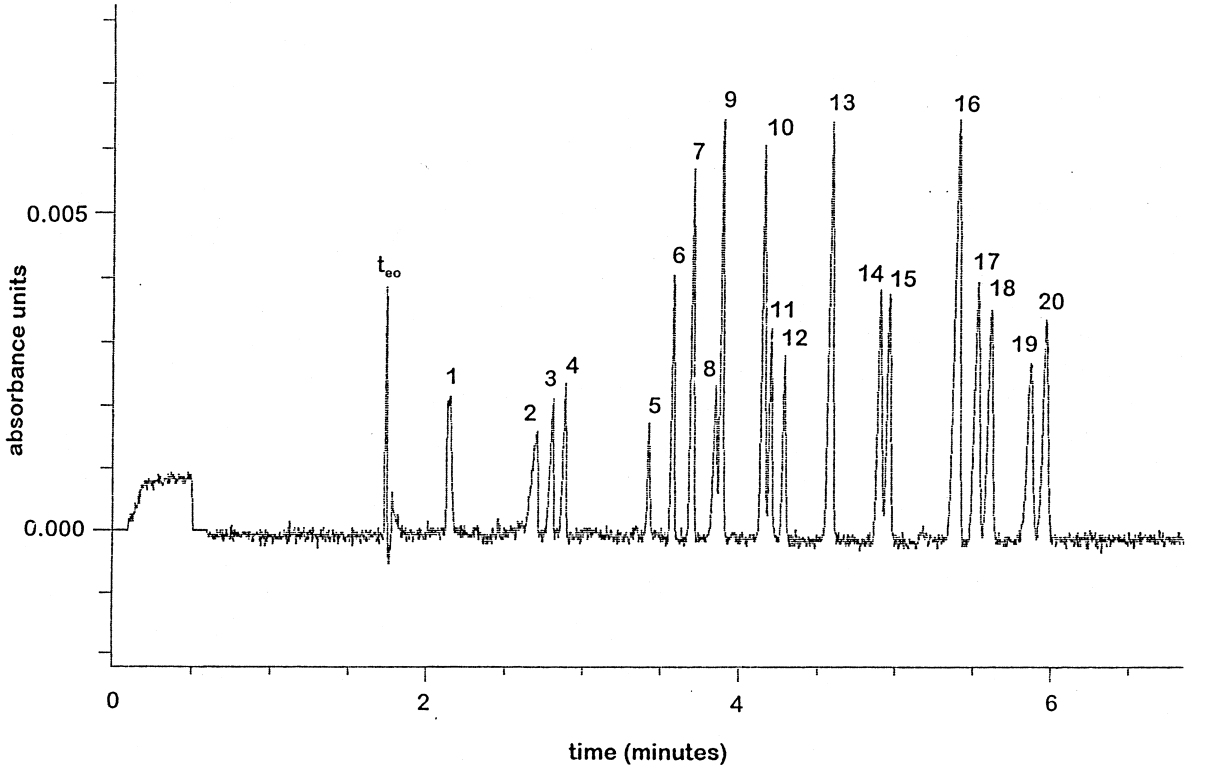

Fig. 8. Separation of phenol and the 19 chlorophenol congeners in 10 m*M* acetic acid+5 m*M* TBAH in ACN. 25 kV→5 μA. Peak identification: (1) phenol, (2) 4-chlorophenol, (3) 2-chlorophenol, (4) 3-chlorophenol, (5) 3,4-dichlorophenol, (6) 2,4-dichlorophenol, (7) 2,3-dichlorophenol, (8) 2,6-dichlorophenol, (9) 3,5-dichlorophenol, (10) 2,5-dichlorophenol, (11) 3,4,5-trichlorophenol, (12) 2,3,4-trichlorophenol, (13) 2,4,5-trichlorophenol, (14) 2,3,5-trichlorophenol, (15) 2,3,4,5-tetrachlorophenol, (16) 2,4,6-trichlorophenol, (17) pentachlorophenol, (18) 2,3,4,6-tetrachlorophenol, (19) 2,3,5,6-tetrachlorophenol, (20) 2,3,6-trichlorophenol.

was extremely pH-sensitive, as very minute changes in the acetic acid/TBAH ratio produced either coelution or changes in elution order among certain pairs of solutes (2,6-dichlorophenol and 3,5-dichlorophenol, for example, coeluted if the buffer was slightly too basic). As long as the buffer composition was kept constant, however, a reproducible elution pattern could be maintained. It is worth noting, though, that after several runs, a uniform drift toward longer migration times was observed, most likely due to interactions between the TBA^+ ion and the capillary wall, which caused a gradual reduction in the electroosmotic flow. In this case, it was necessary to regenerate the capillary with an aqueous sodium hydroxide solution.

The 11 priority pollutants [used in US Environmental Protection Agency (EPA) methods 604, 625/1625 and 8270B] consist of phenols containing both electron withdrawing (chloro and nitro) and electron releasing (methyl) groups. As a result, the phenols in this mixture span a wide pK_a range. The buffer used in the separation of the chlorophenol mixture (10 m*M* acetic acid–5 m*M* TBAH in ACN) could not resolve all the components in the priority pollutant mixture. Lowering the TBAH concentration to 2.5 m*M*, yielded a baseline separation of all 11 components in less than 5 min (Fig. 9). It should be noted that under these conditions, 2,4-dimethylphenol, phenol, 4-chloro-3-methylphenol and 2-chlorophenol (peaks 1, 2, 4 and 5) derive their mobilities from heteroconjugation with the acetate ion, whereas 2-nitrophenol (peak 3) becomes partially deprotonated. This caused the mobility of 2-nitrophenol to become very sensitive to slight

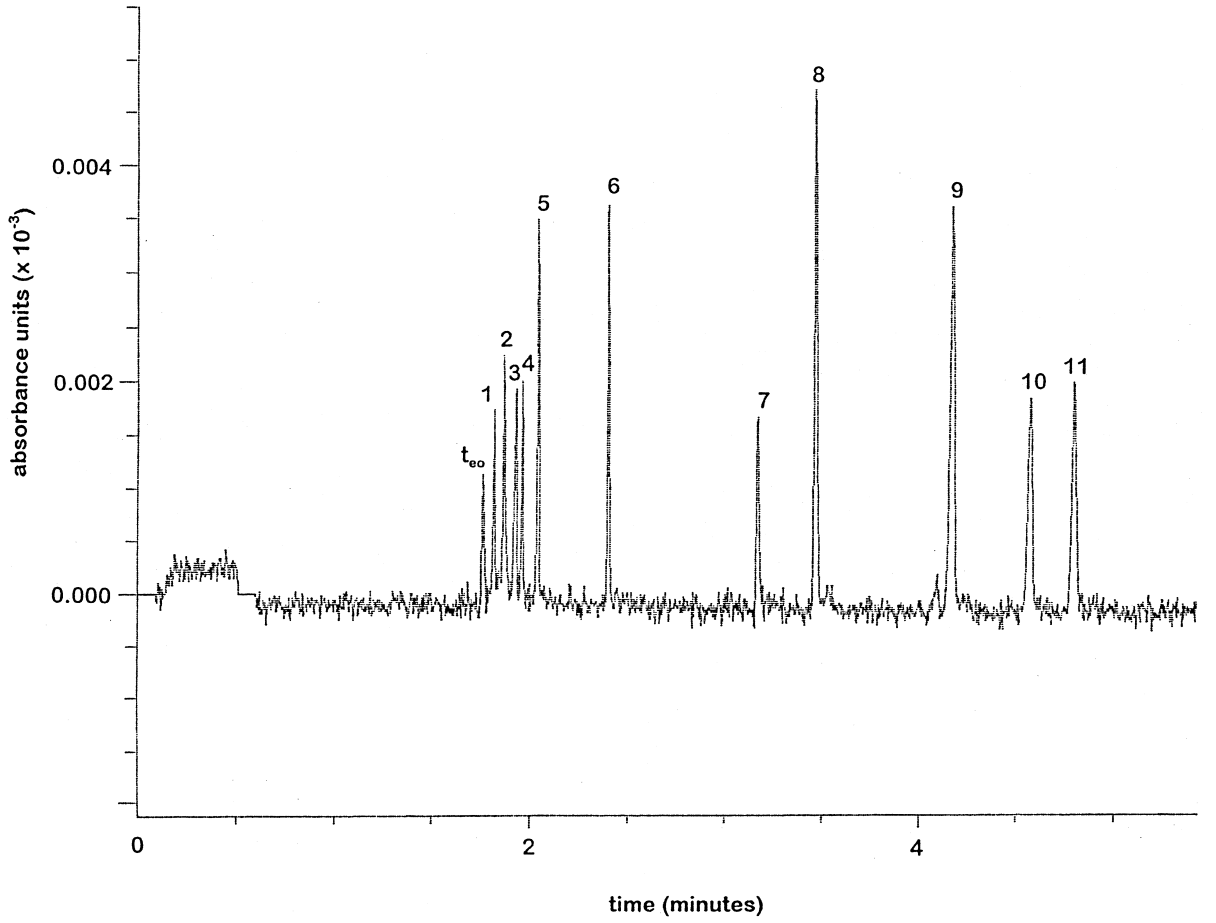

Fig. 9. Separation of the 11 priority pollutant phenols (used in EPA methods 604, 625/1625 and 8270B) in 10 m*M* acetic acid+2.5 m*M* TBAH in ACN. 25 kV→2.3 μA. Peak identification: (1) 2,4-dimethylphenol, (2) phenol, (3) 2-nitrophenol, (4) 4-chloro-3-methylphenol, (5) 2-chlorophenol, (6) 2,4-dichlorophenol, (7) 4-nitrophenol, (8) 2,4,6-trichlorophenol, (9) pentachlorophenol, (10) 4,6-dinitro-*o*-cresol, (11) 2,4-dinitrophenol.

changes in pH, and hence the optimization of our separation centered on the resolution of this component from the surrounding peaks.

4. Conclusion

In NACE separations, the use of a solvent such as ACN allows for separations that are difficult to achieve using other solvents. The reason for this stems from two important properties of ACN. First, its low viscosity leads to shorter analysis times. Second, the moderate polarity of ACN facilitates certain solute–solute interactions that may assist in electrophoretic separations. The combination of heteroconjugation and deprotonation (both of which involve such interactions) was examined, and we found that solutes possessing a wide range of pK_a values (such as the substituted phenols) could be separated rapidly and efficiently using a single ACN-based buffer.

Acknowledgements

Funding by the National Institutes of Health (GM 38738) and the US Environmental Protection Agency is gratefully acknowledged.

References

[1] J.L. Miller, M.G. Khaledi (Eds.), High Performance Capillary Electrophoresis, M.G. Khaledi (Ed.), Chemical Analysis Series, Vol. 146, Wiley, New York, 1998, Chapter 15.
[2] Y. Walbroehl, J.W. Jorgenson, J. Chromatogr. 315 (1984) 135.
[3] C.L. Ng, H.K. Lee, S.F.Y. Li, J. Liq. Chromatogr. 17 (1994) 3847.
[4] G.N.W. Leung, H.P.O. Tang, T.S.C. Tso, T.S.M. Wan, J. Chromatogr. A 738 (1996) 141.
[5] I. Bjørnsdottir, S.H. Hansen, J. Chromatogr. A 711 (1995) 313.
[6] J. Tjørnelund, S.H. Hansen, Chromatographia 44 (1997) 5.
[7] S.H. Hansen, J. Tjørnelund, I. Bjørnsdottir, Trends Anal. Chem 15 (1996) 175.
[8] J. Tjørnelund, S.H. Hansen, J. Chromatogr. A 737 (1996) 291.
[9] I. Bjørnsdottir, S.H. Hansen, S. Terabe, J. Chromatogr. A 745 (1996) 37.
[10] H. Salimi-Moosavi, R.M. Cassidy, Anal. Chem. 68 (1996) 293.
[11] K.D. Altria, S.M. Bryant, Chromatographia 46 (1997) 122.
[12] Y. Walbroehl, J.W. Jorgenson, Anal. Chem. 58 (1986) 479.
[13] Y. Shi, J.S. Fritz, J. High Resolut. Chromatogr. 17 (1994) 713.
[14] P.G. Muijselaar, H.B. Verhelst, H.A. Claessens, C.A. Cramers, J. Chromatogr. A 764 (1997) 323.
[15] J.L. Miller, M.G. Khaledi, D. Shea, Anal. Chem. 69 (1997) 1223.
[16] J.L. Miller, M.G. Khaledi, D. Shea, J. Microcol. Sep. 10 (1998) 681.
[17] J. Tjørnelund, S.H. Hansen, J. Chromatogr. A 792 (1997) 475.
[18] T. Okada, Chem. Commun. (1996) 1779.
[19] T. Okada, J. Chromatogr. A 771 (1997) 275.
[20] C.M. French, I.G. Roe, Trans. Faraday Soc. 49 (1953) 314.
[21] I.M. Kolthoff, S. Bruckenstein, M.K. Chantooni Jr., J. Am. Chem. Soc. 83 (1961) 3927.
[22] J.F. Coetzee, G.R. Padmanabhan, J. Phys. Chem. 69 (1965) 3193.
[23] I.M. Kolthoff, M.K. Chantooni Jr., J. Am. Chem Soc. 87 (1965) 4428.
[24] I.M. Kolthoff, M.K. Chantooni Jr., S. Bhowmik J., J. Am. Chem Soc. 88 (1966) 5430.
[25] I.M. Kolthoff, M.K. Chantooni Jr., J. Am. Chem Soc. 91 (1969) 4621.
[26] I.M. Kolthoff, M.K. Chantooni Jr., in: I.M. Kolthoff, P.J. Elving (Eds.), 2nd ed., Treatise in Analytical Chemistry, Vol. 2, Wiley, New York, 1979, Chapter 19A, and references cited therein.
[27] I.M. Kolthoff, Anal. Chem. 46 (1974) 1992.
[28] S.C. Smith, M.G. Khaledi l.Ch, Anal. Chem. 65 (1993) 193.
[29] B. Ye, M.G. Khaledi, unpublished results, 1994.
[30] N.J. Parekh, L.B. Rogers, J. Chromatogr. 330 (1985) 19.
[31] E. Kenndler, in: M.G. Khaledi (Ed.), High Performance Capillary Electrophoresis, Chemical Analysis Series, Vol. 146, Wiley, New York, 1998, Chapter 2.
[32] A.L. Crego, M.L. Marina, J. Liq. Chromatogr. Rel. Technol. 20 (1997) 1.
[33] K. Otsuka, S. Terabe, T. Ando, J. Chromatogr. 348 (1985) 39.
[34] A. Zemann, D. Volgger, Anal. Chem. 69 (1997) 3243.
[35] M.F. Gonnord, J. Collet, J. Chromatogr. 645 (1993) 327.